

Formation of Nickel-Zinc Ferrite Embedded in a Silica Xerogel Matrix

S. Ponce-Castañeda, J. R. Martínez, S. A. Palomares Sánchez, F. Ruíz, J. A. Matutes-Aquino.

Abstract

We report a study using X-ray diffraction, refinement Rietveld, IR absorption spectroscopy and vibrating sample magnetometry of the formation of particles of Ni-Zn ferrites embedded in a xerogel SiO₂ matrix. Initial solutions were prepared mixing TEOS, distilled water, ethanol, and three different nitrates: iron, nickel and zinc. A molar ratio H₂O:TEOS:Et-OH of 11.66:1.0:4.0 was used in all solutions. Formation of Ni_{0.5}Zn_{0.5}Fe₂O₄ as well as structural modifications of the SiO₂ matrix induced by these particles are discussed. Ni-Zn crystals having dimensions varying from 4 to 16.5 nm have been synthesized by a suitable heat treatment schedule at temperatures varying from 700 to 1100 °C. The coercivity values for different heat-treated samples are found in the range 11–193 Oe, which are significantly larger than those presented by bulk Ni-Zn ferrites.

Keywords: sol-gel, infrared spectroscopy, vibrating sample magnetometry, X-ray diffraction, composites.

Introduction

It is well known that nanophase materials present a variety of interesting magnetic, electric, and catalytic properties which depend strongly on the dimensions of the particles [1–4]. Different systems dispersed in insulating matrices, like silica, have been fabricated by sputter deposition, ball milling, evaporation and chemical methods

[5–8]. These materials presented considerable changes in the magnetic properties when compared with their equivalent pure, bulk materials. For example, ultrafine iron particles having sizes in the range 2–10 nm and embedded in an insulating matrix like SiO₂ exhibit coercivity values two orders of magnitude higher than of bulk iron [9, 10]. Among the wet chemical methods which can be used for the preparation of nanocomposite materials constituted of nanometric metal or metal oxide particles embedded in amorphous silica, the sol-gel process offers some interesting features. In fact, the method depends on many parameters which can be finely modulated in order to lead the process toward the desired final results.

We deal in this paper with the structural and magnetic study by FTIR spectroscopy, x-ray diffraction, vibrating sample magnetometry and Le Bail's method as a variation of the Rietveld refinement [11], of xerogels mixed with iron, nickel and zinc salts added as precursors to form Ni-Zn ferrites embedded in silica xerogels matrix. Special attention is pointed out in the structural effects caused by the adopted experimental conditions and after-heat treatments at elevated temperatures.

Experimental Method

The starting solutions for the formation of silica xerogel composites were prepared by mixing tetraethyl orthosilicate (TEOS), water, and ethanol. The mole ratios of ethanol to TEOS and water to TEOS were 4:1 and 11.66:1, respectively. Separately, amounts of Fe(NO₃)₃· 9H₂O, Ni(NO₃)₂· 6H₂O and Zn(NO₃)₂· 6H₂O were added to the solution at such amount that the ferrite Ni_{0.5}Zn_{0.5}Fe₂O₄ metal oxide concentration, assuming full metal oxidation, is 30 wt% of the final dried powders.

For its incorporation into the SiO₂ matrix, the nitrates were dissolved in water; a homogenous solutions of all components were obtained by mixing water, nitrates dissolved, ethanol and TEOS for about 15 minutes using a magnetic stirring.

Soft pieces of the gels were obtained after about 48 hr. Those pieces were ground to form a fine powder. For subsequent annealing, the samples were placed in an oven at the desired temperature for 30 minutes in air.

The X-ray diffraction patterns were obtained by a Rigaku 2200 diffractometer equipped with a nickel monochromator using CuK α ($\lambda = 1.54 \text{ \AA}$) radiation. The Infrared (IR) spectra were measured by a FTIR spectrometer Nicolet System model Avatar 360, in the diffuse reflectance (DR) mode, mixing 0.05 gr. of powder sample with 0.3 gr. of KBr. Magnetic characterization was performed using a LDJ 9600 vibrating sample magnetometer at room temperature with $H_{\text{max}} = 16 \text{ KOe}$ in order to obtain magnetic parameters such as saturation magnetization. All measurements were performed at room temperature. The Rietveld refinement of amorphous SiO₂ was performed to investigate the structural phases obtained at elevated temperatures.

Results and discussion

In Fig. 1 we showed X-ray diffraction pattern for the SiO₂ sample added with iron, nickel and zinc nitrates and heat treated at a range of 700°C to 1100°C. At 700°C we can see well defined peaks at positions assigned to iron oxides, in particular at 800°C the peak position coincide with those of magnetite, however the intensity value and the position of the peaks correspond to the nickel-zinc ferrite [3, 12]. At temperature of 1100°C the peaks are sharp and well defined indicating the growth of the cluster. The

interaction with the SiO₂ matrix produces a partial devitrification, indicated by the presence of quartz. The ferrite cluster size estimated using the Scherrer's equation [13] is in the range from 4.0 nm to 16.5 nm for temperatures from 800 °C to 1100 °C.

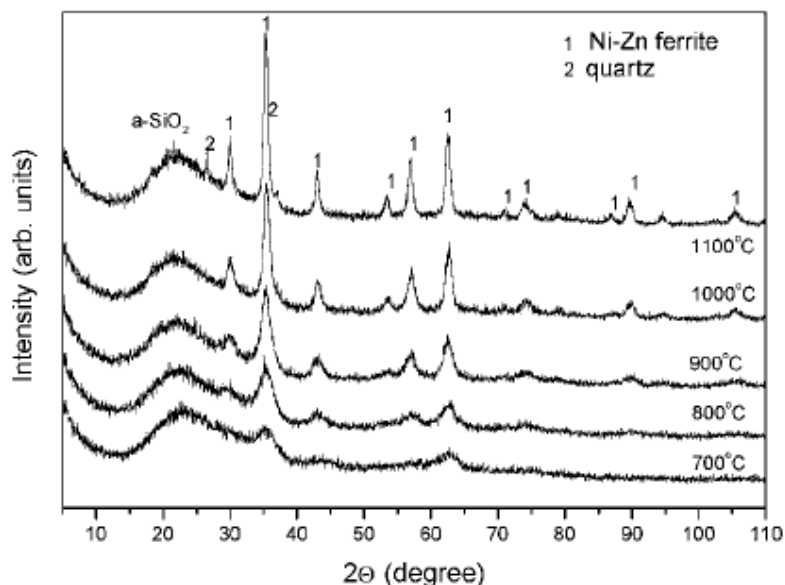


Figure 1. X-ray diffraction patterns for the SiO₂ sample added with iron, nickel and zinc nitrates and heat treated at a range of 700 °C to 1100 °C.

The infrared absorption spectra in the range of 400 cm⁻¹ to 1800 cm⁻¹ obtained on the sample heat treated at the indicated temperatures, are shown in Fig. 2. The three bands identified in the figures with the letters R, B and S correspond to absorption bands related to each particular vibrational mode of the oxygen (O) atom with respect to the silicon (Si) atoms which they bridge. The rocking mode of the O atom along an axis through the two Si atom is associated with the lowest-frequency band centered at about 457 cm⁻¹. The bending mode of the O atom along a line bisecting the axis formed by the two Si atoms corresponds to the band centered at about 800 cm⁻¹. The band at about

1078 cm^{-1} is associated with the asymmetrical stretch motion, in which the O atoms move back and forth along a line parallel to the axis along the two Si atoms [14, 15]. This mode has a strong absorption shoulder at the high energy side. The absorption band at about 950 cm^{-1} is due to vibrations of silanol groups (Si-OH) [16].

From the spectra we can observe a band at 1620– 1650 cm^{-1} assigned to the deformation of molecular water [17]. We can observe that this band has a strong presence on these samples. The presence of this band even at temperatures of 900°C indicates that water still exists in the structural conformation.

In the above mentioned figures it is possible to observe that all the IR spectra show extended well defined bands in the range from about 450 to 770 cm^{-1} ; these bands have been assigned to vibrational modes of Fe O bonds in Fe_2O_3 [18, 19]. These IR features indicate the formation of the iron oxide species at these annealing temperatures.

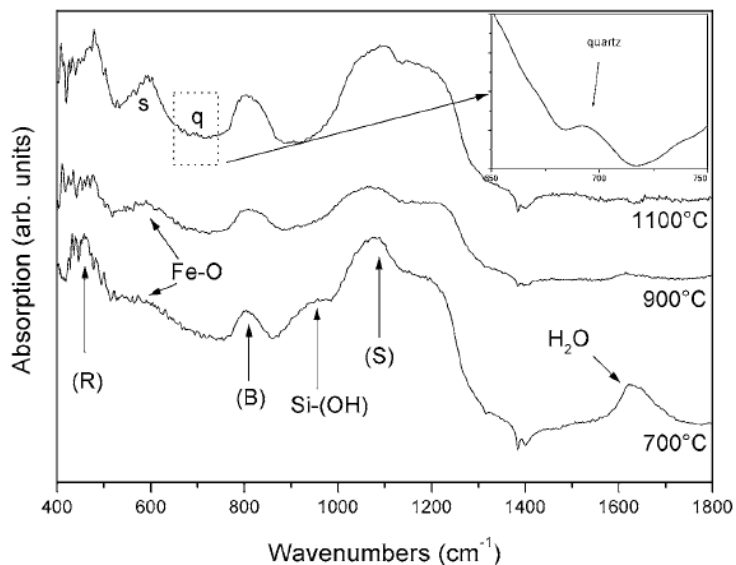


Figure 2. Infrared absorption spectra in the range of 400 cm^{-1} to 1800 cm^{-1} corresponding to sample heat treated at the indicated temperatures.

At 700°C this band is broad and smooth, whereas at temperature above 900°C the band extends only to 669 cm⁻¹ and a peak located at around 570 cm⁻¹ can be observed. This band is associated with the presence of spinel phase. This band is identified in the figure with the letter s. This fact is in accord with X-ray results and indicates that the spinel phase is present at 900°C. At temperature of 1100°C a peak located at about 697 cm⁻¹ assigned to quartz can be observed [20]. This peak is identified in the figure with the letter q.

Special attention has been pointed at the IR absorption spectra for sample treated at 1100°C. In the spectra we can observed that the peaks at about 480 cm⁻¹ are very sharp. This fact and the presence of the peaks at about 420, 557, 620 and 830 cm⁻¹ indicates the formation of spinel phase in accord once with the x-ray results. This formation is accompanied by a structural arrangement of the silica matrix which promotes the appearance of quartz phase. The details can be observed in the Fig. 3 in which we shown a reduced scale of the IR absorption spectrum of the sample heat treated at 1100°C.

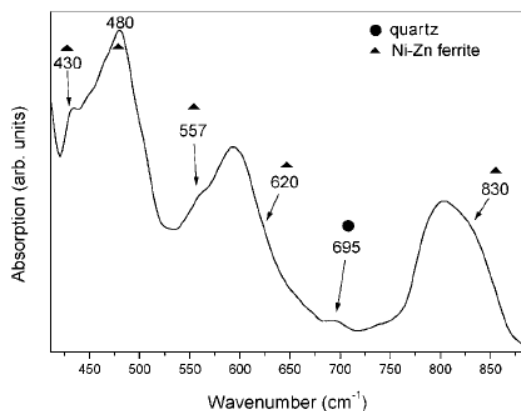


Figure 3. Reduced scale of the IR absorption spectra of the sample heat treated at 1100°C.

The magnetization curves for samples heat treated at the indicated temperatures are shown in Fig. 4. The saturation magnetization increases with the thermal treatment temperature. In the range of temperature analyzed, above 700 °C, the spinel phase start to be formed. In this range the grain size is increased as the annealing temperature is raised, the saturation magnetization increases and the coercivity values decreases.

Figure 5 presents the saturation magnetization and coercivity as a function of the annealing temperature.

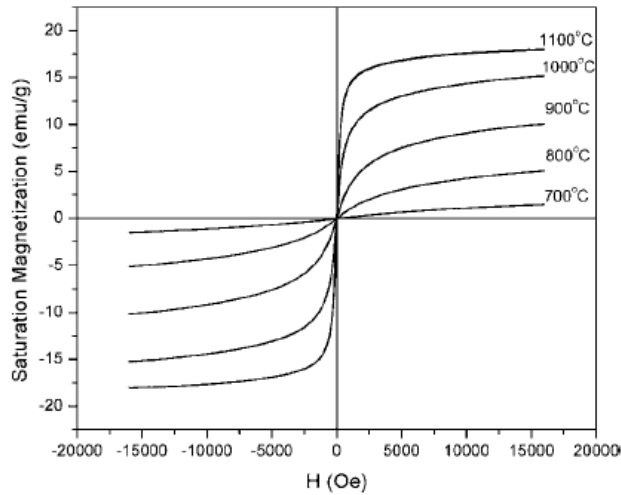


Figure 4. Magnetization curves for samples heat treated at the indicated temperatures.

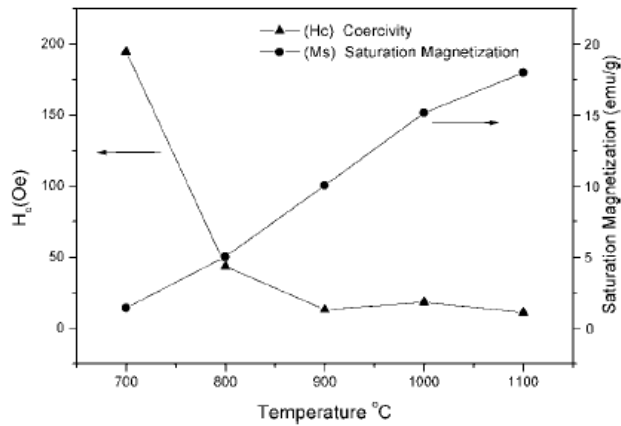


Figure 5. Saturation magnetization and coercivity values as a function of the annealing temperature.

This comportment is in agreement with previous results [3, 21, 22]. It is reported that at 700°C the coercivity starts to decrease, whereas at temperatures lower than 700 °C the coercivity increases when the temperature raises. According to these authors, at 700°C the maximum coercivity is obtained. We present results for a range of heat treatment temperatures from 700°C to 1100°C.

The samples present strong superparamagnetic behaviour due to their small particle sizes. The resulting decrease of saturation magnetization for small particles can be caused by the presence of superparamagnetic relaxation and/or noncolinearity of the magnetic moments at the surface of the nanoparticles [23].

Structural modification of amorphous silica into quartz has been observed at higher temperatures. We believe that the ferrite-glass interface could strongly influence the coercivity of our nanocomposites. Since our samples contain very small particles, a large fraction of ions is at or near the surface so that the interaction between the ferrite particles and the silica matrix may play a determinant role.

The magnetization saturation shown in Fig. 5 does not attain saturation at the highest magnetic field of 16 kOe used in our measurements.

The magnetic parameters for the sample heat treated at 1000°C show a little change in their hysteresis loop. This situation is related to a structural change produced by the interaction of the ferrite nanocluster with the silica gel matrix. At this temperature start to appear crystallite quartz for the matrix and a well defined crystallite ferrite phase.

The presence of this three phases at this temperature, is corroborated by the Rietveld refinement for amorphous SiO₂, introduced by Le Bail [11]. From a fit of measured X-ray diffraction data by theoretical intensities the crystal structure can be refined on the basis of an initial assumption for the structure.

Using the above Rietveld process the Bragg pattern and the peak positions of the diffractograms corresponding to the phases identified accord to the spatial group Fd-3m

for Ni-Zn ferrite, P6₂22 for the quartz and P4₁2₁2 for the low cristobalite, have a good coincidence.

The spatial group used for the low cristobalite is representative for the amorphous phase. This fact is justified by the results shown in the X-ray diffractogram of the Fig. 1, for the amorphous band associated to the SiO₂. The main feature of these patterns is a broad band located at the left part of the diffractogram. According to the treatment temperature, this band suffers a slight shift to lower degrees. For the sample heat treated at 700 °C the position of the centre is around 23.13 degrees, and for higher temperatures (1100 °C) the peak is located at 21 degrees. It is important to mention that cristobalite has its main diffraction peak at this position (21 °). Many authors have correlated the shift, induced by temperature, of this broad band to the structural conformation of the silica matrix.

Conclusions

Using the sol-gel method we have synthesised particles of Ni_{0.5}Zn_{0.5}Fe₂O₄ embedded in a silica xerogel matrix. The coercivity values for these nanocomposites are in the range 11–193 Oe, which are significantly larger than those presented by bulk Ni-Zn ferrites. This increased in the coercivity is ascribed to small sizes of the particles. The formation of the Ni-Zn ferrite conduce to the structural rearrangement of the silica xerogel matrix very close to the quartz phase. At temperatures about 1000 °C the interaction of the matrix with the embedded phase conduce a variation in the magnetic parameters. At 1100 °C exist a coexistence of the Ni-Zn ferrite, the amorphous phase and the quartz phase, which was corroborated by the Rietveld refinement.



Acknowledgments

This work was done under the auspices of CONACYT (México) through grants G-25851-E and W-8001 (Millenium initiative)

References

1. E. Kroll, F.M.Winnik, and R. Ziolo, *ChemMater.* **8**, 1594 (1996).
2. C. Cannas, D. Gatteschi, A. Musinu, G. Piccaluga, and C. Sangregorio, *J. Phys. Chem. B* **102**, 7721 (1998).
3. M. Pal, D. Das, S.N. Chintalapudi, and D. Chakravorty, *J. Mater. Res.* **15**, 683 (2000).
4. C. Mirkin, R. Letsinger, R. Mucic, and J. Storhoff, *Nature* **382**, 607 (1996).
5. C.L. Chien, *Ann. Rev. Mater. Sci.* **25**, 129 (1995).
6. G. Xiao, S. Liou, A. Levy, J. Taylor, and C.L. Chien, *Phys. Rev. B* **34**, 7573 (1986).
7. C. Estournes, T. Lutz, J. Happich, T. Quaranta, P. Wissler, and J. Guill, *J. Magn. Mater.* **173**, 83 (1997).
8. L. Zhang, G.C. Papaefthymiou, R.F. Ziolo, and J.Y. Ying, *Nanostruct. Mater.* **9**, 185 (1997).
9. G. Xiao and C.L. Chien, *Appl. Phys. Lett.* **51**, 1280 (1987).
10. S.H. Liou and C.L. Chien, *Appl. Phys. Lett.* **52**, 512 (1988).
11. A. Le Bail, *J. Non-Cryst. Solids* **183**, 39 (1995).
12. International Center for Diffraction Data, *Inorganic Phases* (Joint Committee on Powder Diffraction Standards, Swarthmore,



- PA, 1995), Power Diffraction File, Card Nr. 08-0234.
13. B.E.Warren, *X-ray Diffraction* (Addison-Wesley, Reading, MA, 1980), p. 253.
14. P. Sen and M.F. Thorpe, Phys. Rev. B **15**, 4030 (1979).
15. F.L. Galeener, Phys. Rev B **15**, 4292 (1979).
16. A. Duran, C. Serna, V. Fornes, and J.M. Fern´andez-Navarro, J. Non-Cryst. Solids **63**, 45 (1984).
17. N.B. Colthup, L.H. Daly, and S.E. Wiberly, *Introduction to Infrared and Raman Spectroscopy*, 2nd edn. (Academic Press, New York, 1975).
18. K. Kandori, N. Ohkoshi, A.Yasukawa, and T. Ishikawa, J.Mater. Res. **13**, 1698 (1998).
19. Liping Li, Guangshe Li, R.L. Smith Jr., and H. Inomata, Chem. Mater. **12**, 3705 (2000).
20. F. Gervais and B. Piriou, Phys. Rev. B **11**, 3944 (1975).
21. A. Chatterjee, D. Das, S.K. Pradhan, and D. Chakravorty, J. Magn. Magn. Mater. **127**, 214 (1993).
22. A.S. Alburqueque, J.D. Ardisson, and W.A.A. Macedo, J. Magn. Magn. Mater. **192**, 277 (1999).
23. K. Haneda and A.H. Mor´is, J. Appl. Phys. **63**, 4258 (1988).